



Methodological considerations in assessing counter-movement jumps with handheld accentuated eccentric loading

Thomas E. Bright, John R. Harry, Jason Lake, Peter Mundy, Nicola Theis & Jonathan D. Hughes

To cite this article: Thomas E. Bright, John R. Harry, Jason Lake, Peter Mundy, Nicola Theis & Jonathan D. Hughes (11 Jul 2024): Methodological considerations in assessing counter-movement jumps with handheld accentuated eccentric loading, Sports Biomechanics, DOI: [10.1080/14763141.2024.2374884](https://doi.org/10.1080/14763141.2024.2374884)

To link to this article: <https://doi.org/10.1080/14763141.2024.2374884>



© 2024 The Author(s). Published by Informa UK Limited, trading as Taylor & Francis Group.



Published online: 11 Jul 2024.



Submit your article to this journal [↗](#)



Article views: 403



View related articles [↗](#)



View Crossmark data [↗](#)

Methodological considerations in assessing countermovement jumps with handheld accentuated eccentric loading

Thomas E. Bright ^{a,b}, John R. Harry ^c, Jason Lake ^d, Peter Mundy ^e, Nicola Theis ^f and Jonathan D. Hughes ^a

^aCardiff School of Sport and Health Sciences, Cardiff Metropolitan University, Cardiff, UK; ^bSchool of Sport, Exercise and Rehabilitation, Plymouth Marjon University, Plymouth, UK; ^cHuman Performance & Biomechanics Laboratory, Department of Kinesiology & Sport Management, Texas Tech University, Lubbock, TX, USA; ^dInstitute of Sport, Nursing, and Allied Health, University of Chichester, Chichester, UK; ^eResearch and Development, Hawkin Dynamics, Inc, Westbrook, ME, USA; ^fSchool of Sport and Exercise, University of Gloucestershire, Gloucester, UK

ABSTRACT

This study aimed to compare the agreement between three-dimensional motion capture and vertical ground reaction force (vGRF) in identifying the point of dumbbell (DB) release during a countermovement jump with accentuated eccentric loading (CMJ_{AEL}), and to examine the influence of the vGRF analysis method on the reliability and magnitude of CMJ_{AEL} variables. Twenty participants (10 male, 10 female) completed five maximal effort CMJ_{AEL} at 20% and 30% of body mass (CMJ_{AEL20} and CMJ_{AEL30}, respectively) using DBs. There was large variability between methods in both loading conditions, as indicated by the wide limits of agreement (CMJ_{AEL20} = -0.22 to 0.07 s; CMJ_{AEL30} = -0.29 to 0.14 s). Variables were calculated from the vGRF data, and compared between four methods (forward integration (FI), backward integration (BI), FI adjusted at bottom position (BP), FI adjusted at DB release point (DR)). Greater absolute reliability was observed for variables from DR (CV% ≤ 7.28) compared to BP (CV% ≤ 13.74), although relative reliability was superior following the BP method (ICC ≥ 0.781 vs ≥ 0.606, respectively). The vGRF method shows promise in pinpointing the DB release point when only force platforms are accessible, and a combination of FI and BI analyses is advised to understand CMJ_{AEL} dynamics.

ARTICLE HISTORY

Received 3 April 2024
Accepted 27 June 2024

KEYWORDS

Countermovement jump; accentuated eccentric loading; 3D motion capture; force platform; numerical integration

Introduction

The integration of accentuated eccentric loading (AEL) into vertical jump training is a popular method among sports scientists and strength and conditioning coaches to enhance lower-body force production capabilities in stretch-shortening cycle (SSC) exercises (Bright et al., 2023; Merrigan et al., 2022; Wagle et al., 2017). This training method is most commonly applied to a countermovement jump (CMJ_{AEL}) or drop jump

CONTACT Thomas E. Bright  tommybright55@gmail.com

© 2024 The Author(s). Published by Informa UK Limited, trading as Taylor & Francis Group.

This is an Open Access article distributed under the terms of the Creative Commons Attribution License (<http://creativecommons.org/licenses/by/4.0/>), which permits unrestricted use, distribution, and reproduction in any medium, provided the original work is properly cited. The terms on which this article has been published allow the posting of the Accepted Manuscript in a repository by the author(s) or with their consent.

(DJ_{AEL}) and involves the use of additional mass, which is held during the countermovement and released immediately before the propulsion phase (Handford et al., 2021). Given that muscular force is greater when a concentric action is preceded by an eccentric action, the additional mass accrued through AEL is thought to add to the potentiating effect of the SSC component of a CMJ (Sheppard et al., 2007; Su et al., 2023a, 2023b).

During a CMJ, the additional mass and loading of the hip and knee extensors will amplify the pre-stretch state of muscle tissue, leading to increased force production in the propulsion phase (Bosco et al., 1982; Finni et al., 2001; Hahn et al., 2007; Komi & Gollhofer, 1997). However, the precise mechanisms behind this enhancement remain to be fully elucidated. Past investigations have attributed AEL performance effects to factors such as improved elastic strain energy storage and release in the tendon and aponeurosis (Wiesinger et al., 2017). Nonetheless, recent evidence has challenged these assumptions (Su et al., 2023a, 2023b), prompting a need for a more comprehensive understanding of the coordination strategies and biomechanical changes induced by AEL during maximal CMJ performance. Addressing this requires consideration of a number of methodological issues.

The first is the assumption that the release of additional mass takes place at the lowest point of the countermovement (i.e., peak negative displacement). However, existing studies have not systematically quantified this point (Aboodarda et al., 2013; Harrison et al., 2019; Taber et al., 2023), leading to reliance on an unsubstantiated belief of current coaching practices being sufficient to achieve this. Understandably, assuming the additional mass is released at the bottom position is necessary to uphold the theorised mechanisms and coordination strategy of the jump. Premature release may result in under-potentialisation of the aforementioned mechanisms, while a delayed release could lengthen the amortisation phase and disrupt an athlete's coordination strategy during the transition to the propulsion phase (Frayne et al., 2021). It is therefore imperative to ensure that the additional mass is held throughout the countermovement and released as close to an athlete's lowest position as possible. While an accurate measurement of this point could be achieved through three-dimensional (3D) motion capture, practical considerations, including cost and the difficulty of equipment setup and analysis, make this approach impractical for widespread use. Therefore, a method of identifying the release using vertical ground reaction force (vGRF) data extracted from force platforms is appealing for practitioners.

The second issue arises from the use of force platforms to understand AEL performance (Aboodarda et al., 2013; Bridgeman et al., 2016; Gross et al., 2022; Lloyd et al., 2022; Su et al., 2023b; Taber et al., 2023). When computing the whole-body centre of mass (CoM) using vGRF data, Newton's Second Law is applied to determine acceleration. Subsequently, this acceleration is integrated once to derive CoM velocity and then again to calculate CoM displacement (Gard et al., 2004). The mass for these calculations is usually recorded from an average of the static vGRF at the start of the movement (McMahon et al., 2018; Street et al., 2001). However, this approach introduces potential sources of error, including force platform noise (i.e., sensor drift, low-frequency noise, temperature fluctuations, cross talk, and non-linearity due to electronic errors) and vGRF fluctuations resulting from slight movements by the participant (Psycharakis &

Miller, 2006; Quagliarella et al., 2008; Zok et al., 2004). A recent study substantiated previous findings (Kibele, 1998; Street et al., 2001) by indicating that a 1 kg mass change identified in the weighing phase led to a 7.7 cm change in CMJ jump height, accompanied by significant changes in starting versus landing and final positions (Burnett et al., 2023). These errors, observed in investigations where the mass remains constant or changes by a small margin, are likely exacerbated in the context of a CMJ_{AEL} due to the substantial change of mass at the point of release. Given that computed CoM velocity and displacement are involved in determining outcome variables used to assess the effect of AEL on performance (Aboodarda et al., 2013; Harrison et al., 2019), meticulous consideration of the error magnitude is essential.

The third issue involves the analysis techniques used to determine outcome variables. For example, in situations where the initial weighing phase at the start of a jump is missing, as seen in drop jumps, researchers have utilised a technique known as backward integration (BI) (Grozier et al., 2021; Wade et al., 2022; Wank & Coenning, 2019). This technique mirrors forward integration (FI), but with a notable distinction: rather than integrating from the initial standing period and across the countermovement and propulsion phases, the process initiates from the standing period after the landing phase. Given that a jump begins and concludes in a state of quiet standing, with all the energy generated to elevate the CoM needing to be dissipated upon landing, this method enables calculation of jump height and other performance metrics. Recent work has found this method to be valid for calculating both maximal and submaximal CMJ heights, albeit contingent on the assumption that athletes quickly return to an upright and still position upon landing (Wade et al., 2022). In the context of a CMJ_{AEL} , exclusively employing FI without accounting for the change in mass will likely introduce significant errors in CoM velocity, displacement and any further calculations made (i.e., jump height and countermovement depth), particularly given the lack of data on when the additional mass is actually released and whether this is consistent. Similarly, reliance on BI alone is inadequate if the objective is to accurately understand the entire movement. Hence, a synergistic application of both FI and BI methods appears optimal for CMJ_{AEL} analyses.

Ensuring the reliable measurement of CMJ_{AEL} through vGRF data alone is important, given the widespread use of force platforms in research and practice. Therefore, the aims of the study were to (1) find a method of quantifying dumbbell (DB) release without the need for advanced data acquisition devices (i.e., 3D motion capture) and (2) determine a method through which information can be reliably extracted and analysed during a CMJ_{AEL} from force-time data alone. To validate these considerations, we hypothesised that the agreement between motion capture and vGRF methods of identifying the dumbbell release point would meet acceptable standards for CMJ_{AEL20} and CMJ_{AEL30} (additional DB load at 20% and 30% of body mass, respectively). Additionally, it was hypothesised that force-time variables extracted from CMJ_{AEL20} and CMJ_{AEL30} using FI and BI analysis techniques would display significant differences.

Materials and methods

Participants

Twenty participants (10 men and 10 women; age: 23.5 ± 4.2 years; height: 1.7 ± 0.1 m; body mass: 74.2 ± 16.5 kg) volunteered to participate in this study. All participants were classified as recreationally active according to their participation in recreational sports and exercise involving the CMJ (\geq two times per week) for at least six months prior to participation. All were free from any previous musculoskeletal injuries within the last year and from any neuromuscular disorders that would affect their ability to complete data collection. Written informed consent was obtained prior to the study commencing. Ethical approval was granted by the institutional ethics committee at the site of data collection in accordance with the declaration of Helsinki.

Testing procedures

Participants were invited into the biomechanics laboratory on one occasion for data collection. Age, height, body mass and sex were recorded, and a demonstration of the testing protocol was provided. Before jump testing, participants performed a standardised dynamic warm-up and familiarisation. This began with 5 min of stationary cycling at a self-selected pace followed by 10 body weight squats, 10 jump squats, and 20 forward step walking lunges. Participants then performed up to five CMJ_{AEL} trials that were progressed in perceived intensity from moderate to maximum effort and interspersed by approximately 30 s of rest. The research team visually inspected jumps to ensure correct technical execution.

Following completion of the warm-up, participants underwent two experimental conditions in a randomised order: a) five trials of CMJ_{AEL} with DBs at 20% of body mass (CMJ_{AEL20}, a DB of 10% of body mass in each hand) and b) five trials of CMJ_{AEL} with at 30% of body mass (CMJ_{AEL30}, a DB of 15% of body mass in each hand). The CMJ_{AEL} loads selected were based on previous investigations (Aboodarda et al., 2013, 2014; Bridgeman et al., 2016; Gross et al., 2022; Su et al., 2023b). Participants were provided with the following instructions: *'perform the countermovement at your maximum comfortable speed, release the dumbbells at your lowest position before moving upward and continue to jump as fast and as high as possible'*. These instructions were chosen to prevent participants from purposefully releasing the DBs before or after their lowest position and subsequently altering the fluidity of the movement. After releasing the DBs, participants were cued to return their arms to the akimbo position for the remainder of the jump and landing. One-minute rest was allocated between each trial, with 3 min of rest between conditions.

Equipment

Data from each trial were captured using two parallel force platforms (OPT464508; Advanced Mechanical Technology, Inc., Watertown, MA, USA) embedded in the laboratory floor and a 12-camera 3D motion capture system (Vantage v5 cameras; Vicon Motion Systems, Ltd., Oxford, UK) synchronously sampled at 2000 Hz and 200 Hz, respectively. Spherical 14 mm retro-reflective

markers were placed bilaterally over the following anatomical locations: acromion process, C7 vertebrae, sternum-clavicular notch, xiphoid process, 10th thoracic vertebrae, iliac crest, anterior superior iliac spine, posterior superior iliac spine, sacrum, greater trochanter, medial and lateral femoral epicondyles, medial and lateral tibial condyles, medial and lateral malleoli, calcaneus, and the first and fifth metatarsal heads. In addition, four markers were secured on the medial and lateral sides of each end of the DBs to form a rectangular-shaped segment (Figure 1). Data were collected using Vicon Nexus software (v2.14; Vicon Motion Systems, Ltd., Oxford, UK).

Data analysis

Visual3D biomechanical software (HAS-Motion, Inc., Germantown, MD) was used for data processing. Raw vGRF signals from the two force platforms were summed to represent the vGRF acting at the whole-body CoM. The raw marker trajectories were used to create a model that included trunk and pelvis segments in addition to thigh, leg, foot, and DB segments bilaterally. The total vGRF signal and marker trajectories were then smoothed using a fourth-order, bidirectional, low-pass Butterworth digital filter with cut-off frequencies of 10 Hz and 50 Hz, respectively. These cut-off frequencies were determined by collecting pilot data and transforming the raw kinematic and kinetic data from the time domain to the frequency domain (Fast Fourier Transform). The transformed data was subsequently visually inspected to identify the frequency range where the majority of the signal was situated (Harry et al., 2022). The vGRF and DB position

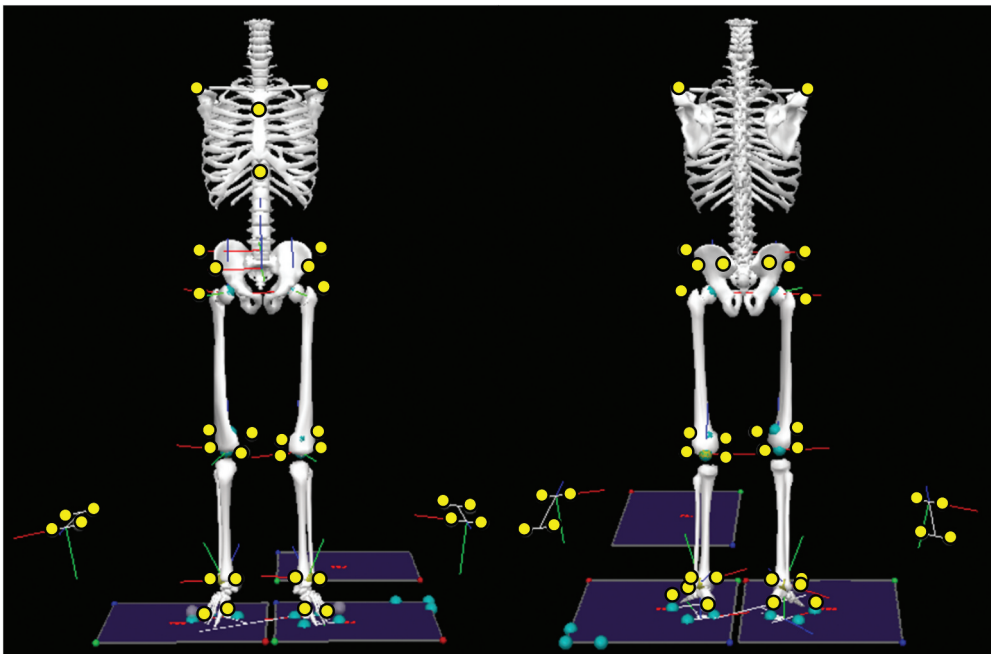


Figure 1. Locations of the 28 single reflective markers that were adhered on the participants body and 8 single reflective markers that were placed on the dumbbells.

data were processed to create time-histories for the following variables: summed vGRF, Model CoM, and DB CoM, which were exported to MATLAB for further analysis (R 2022b; The Mathworks, Inc., Natick, MA, USA) and downsampled to match the sampling frequency of the motion capture system (200 Hz). This enabled detailed analyses of the vGRF and motion curves to locate the exact point of DB release, which required FI and BI processes due to the changes of system weight that compromises the accuracy of the integrations after the DBs' release.

Forward integration

System weight, representing bodyweight + DB, was obtained by averaging one second of the vGRF signal at the start of the jump (weighing period) as the participants stood motionless while awaiting the command to jump (i.e., '3,2,1, jump!'). The weighing period was used to ensure an initial velocity of zero and to identify the vGRF maximum, minimum and standard deviation (SD) during this phase. The start of the movement was then defined as the first occurrence in which the maximum force during the weighing period exceeded system weight + five times the SD during this phase (pre-load strategy), or it dropped below the minimum—five SD (unload strategy). Net vGRF (vGRF—system weight) was divided by system mass to calculate CoM acceleration. The CoM acceleration was integrated using the trapezoidal rule to obtain CoM velocity, which was then integrated to calculate CoM displacement (Figure 2) (Owen et al., 2014). Integration began at the start of the weighing period, with data subsequently cropped to begin at this point.

The braking phase began one sample after the lowest countermovement CoM velocity occurred and ended one sample after the first occurrence of a CoM velocity of 0 m/s

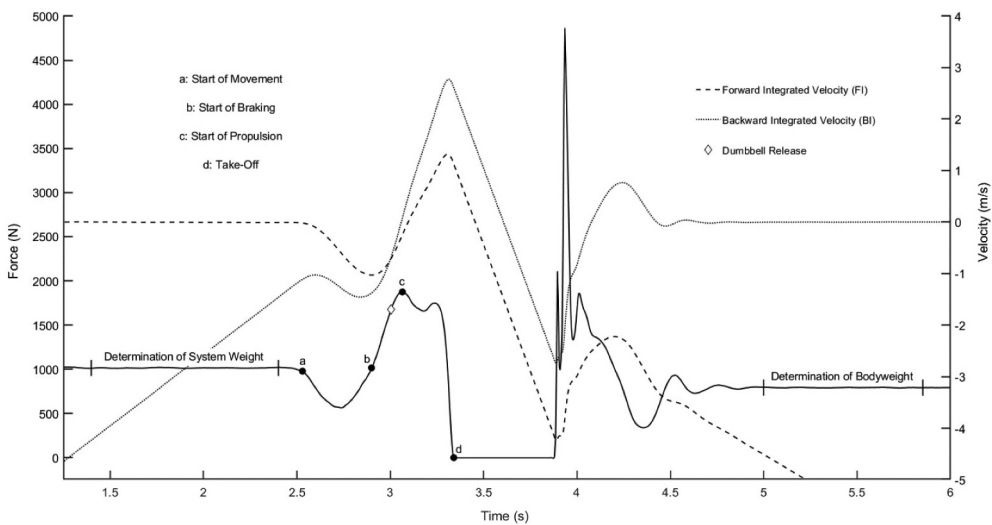


Figure 2. Force-time signal for a countermovement jump with accentuated eccentric loading. Velocity-time signals, derived from forward integration (FI; dash-dot black line) and backward integration (BI; dashed black line), are also presented and the start of movement, dumbbell release, braking, propulsion, and take-off points highlighted.

(McMahon et al., 2018). This also coincided with the beginning of the propulsion phase, which ended at take-off (identified using a 10 N threshold). Likewise, ground contact was defined using a 10 N threshold.

The following variables were extracted using the FI data: jump height (JH), derived from velocity at take-off; reactive strength index modified (RSI_{mod}), calculated as JH divided by time to take-off (TTO), countermovement depth, defined as the change in displacement between the start of movement and the end of the braking phase and the time duration, mean force and velocities during the braking and propulsion phases.

Backward integration

The vGRF signal was flipped using MATLABs ‘flipud’ function such that the first recorded data point became the last data point in the time-history. Then, bodyweight was calculated from approximately one second of the post-landing period where participants were instructed to return to an upright and motionless position as quickly as possible (Wade et al., 2022). The post-landing period was used to ensure an initial velocity of zero and to identify the vGRF maximum, minimum and SD. The end of landing was then defined as the first occurrence in which bodyweight exceeded either the maximum vGRF + five SD or the minimum vGRF—five SD. The FI methods were then repeated by calculating CoM acceleration, performing integration to obtain CoM velocity and once more to get CoM displacement (Owen et al., 2014). Finally, the CoM acceleration, velocity and displacement signals were flipped to match the original direction of the vGRF signal (Figure 2).

The change of mass as a result of DB release is not likely to impact the vGRF signal; therefore, take-off and ground contact locations remained unchanged. However, the end of the braking phase was re-calculated using the CoM velocity obtained through BI. This was done as the authors’ have found that the CoM velocity will be accurate through FI up until the point that DBs are released and equally, CoM velocity through BI will be accurate until the point in which DBs contact the hands (working backwards through the movement). The same variables calculated in the FI section were repeated using the BI data.

Dumbbell release point

The DB release point was identified through 3D motion capture and vGRF data. First, the right DB segment position data was differentiated to obtain DB velocity and then acceleration. The difference between this signal and the CoM acceleration (FI) was then calculated as DB acceleration—CoM acceleration. The DB release point was identified as the first value in this signal that exceeded a value of 2 m/s^2 (Figure 3). This was selected based on prior observations in Vicon Nexus Software and Visual 3D, and pilot studies indicating that this threshold reliably corresponds to the onset of the release as the hands begin to open.

Using the vGRF data, the DB release point was located as the instance in which FI and BI CoM velocity intersected. This was chosen as it represents the instant at which the two masses (i.e., system mass and body mass) became equal as they transition to take each other’s magnitude. Visual inspection of the data in Visual 3D also confirmed this assumption.

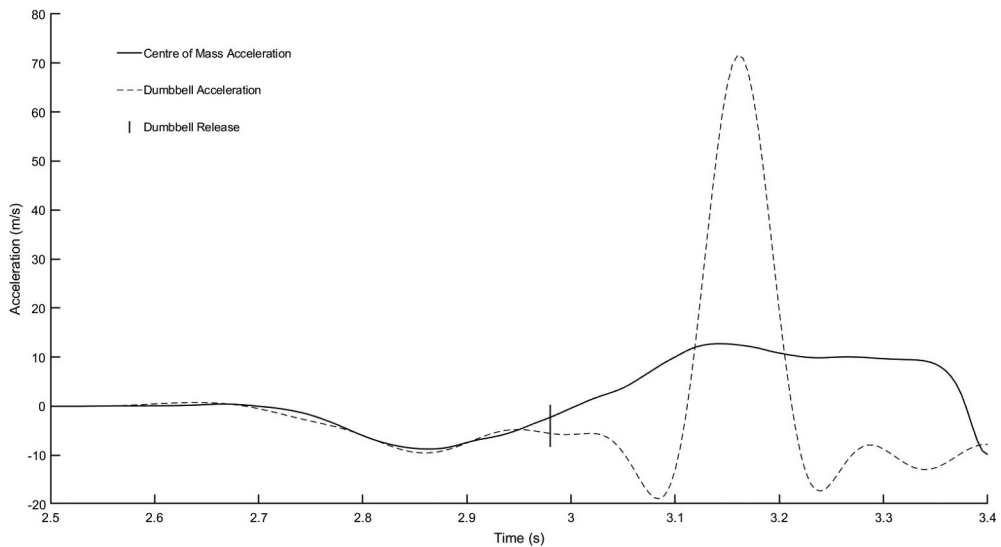


Figure 3. Centre of mass acceleration (solid black line) and dumbbell acceleration (dashed black line) signals plotted to highlight the dumbbell release point as occurring at the location in which these signals differ by ≥ 2 m/s (vertical solid black line).

Adjusting forward integration

To facilitate comparisons with previous investigations (Harrison et al., 2019; Taber et al., 2023), we also calculated CoM velocity and displacement signals whereby system mass was changed to body mass at the braking end point (BP) and DB release point (DR). This involved calculating CoM acceleration until the BP and DR using system mass before manually changing to body mass thereafter. The braking and propulsion start points were subsequently calculated using the methods outlined above. Take-off and ground contact locations were taken from the data calculated previously.

JH, RSI_{mod} and countermovement depth calculations were repeated for BP and DR methods. Because FI and BP variables would be identical for data extracted from the braking and propulsion phase, only DR was used to obtain braking and propulsion times, mean force and velocity for comparisons.

Statistical analysis

Agreement between the 3D motion capture and vGRF approaches to identify the DB release point was examined using repeated measures Limits of Agreement analysis to ensure that the SD's were not underestimated (Bland & Altman, 2007). For each timepoint, this method calculates the SD, and subsequently the upper and lower limits of agreement (LOA), using total variance across all data points from a one-way analysis of variances (ANOVA) (participant and residual mean square scores). To account for uncertainty in the estimates and provide the precision of the estimated agreement between the two approaches, 95% confidence intervals (CI_{95}) were computed for the mean bias and upper and lower LOA (Hamilton & Stamey, 2007).

A detailed guide and rationale for the repeated measures Limits of Agreement analysis was recently reported (Wade et al., 2023). We could not determine an *a priori* literature-based criterion for adequate agreement (i.e., bias) because of a lack of similar investigations. Therefore, we defined agreement using a bias threshold of ± 0.05 s, which was based upon adjusting the mass at different time points and examining the subsequent magnitude of error in the CoM velocity and displacement data. It is also worth noting that this threshold is within the time delay (± 0.08 s) experienced between the participants' lowest position and the release of additional mass in a recent study (Su et al., 2023b).

A two-way repeated measures ANOVA (method [FI, BI, BP, DR] x load [CMJ_{AEL20}, CMJ_{AEL30}]) was conducted to compare the differences between dependent variables. The Greenhouse–Geisser correction was used when the Mauchly's sphericity test was violated and pairwise differences were identified using Bonferroni post-hoc corrections. Effect sizes were calculated using Hedges' *g* method, providing a measure of the magnitude of the differences in each variable noted between time points, and were interpreted as trivial (≤ 0.19), small (0.20 to 0.49), moderate (0.50 to 0.79) or large (≥ 0.80) (Cohen, 2009).

A two-way random effects model (absolute agreement, average measures) intraclass correlation coefficient (ICC), along with upper and lower CI₉₅, were used to determine the relative reliability. Based on the lower CI₉₅ of the ICC estimate, values were interpreted as: <0.5 , poor; 0.5 to 0.75, moderate, 0.75 to 0.90, good and >0.90 , excellent (Koo & Li, 2016). Absolute reliability was assessed using the coefficient of variation (CV%), which was calculated via the root mean square approach (Hyslop & White, 2009). To provide a qualitative scale in line with the ICC estimates, CV% thresholds of $<5\%$, 5% to 10%, 10% to 15% and $>15\%$ (based on the upper CI₉₅) were considered to represent excellent, good, moderate and poor reliability, respectively.

The ICC estimates, two-way repeated measures and one-way ANOVA were performed in SPSS (version 28.0; SPSS Inc., Chicago, IL, USA), and statistical significance was accepted at $p \leq 0.05$. All other analyses were performed in Microsoft Excel (version 2311, Microsoft Corp., Redmond, WA, USA).

Results

Three participants' data were omitted from the final analysis due to issues surrounding the weighing and/or post-landing period. Therefore, the final sample consisted of 17 participants (nine men and eight women; age: 23.1 ± 2.7 years; height: 1.7 ± 0.1 m; body mass: 75.1 ± 17.4 kg).

Agreement

Figure 4 and 5 present the agreement between the motion capture and vGRF methods used to identify the DB release point location for CMJ_{AEL20} and CMJ_{AEL30}, respectively. Table 1 provides the bias, SD of bias, upper and lower LOA and CI₉₅ for both conditions. The agreement between methods was unacceptable in both loading conditions, as evidenced by the large LOA (CMJ_{AEL20} = -0.22 to 0.07 s; CMJ_{AEL30} = -0.29 to 0.14 s).

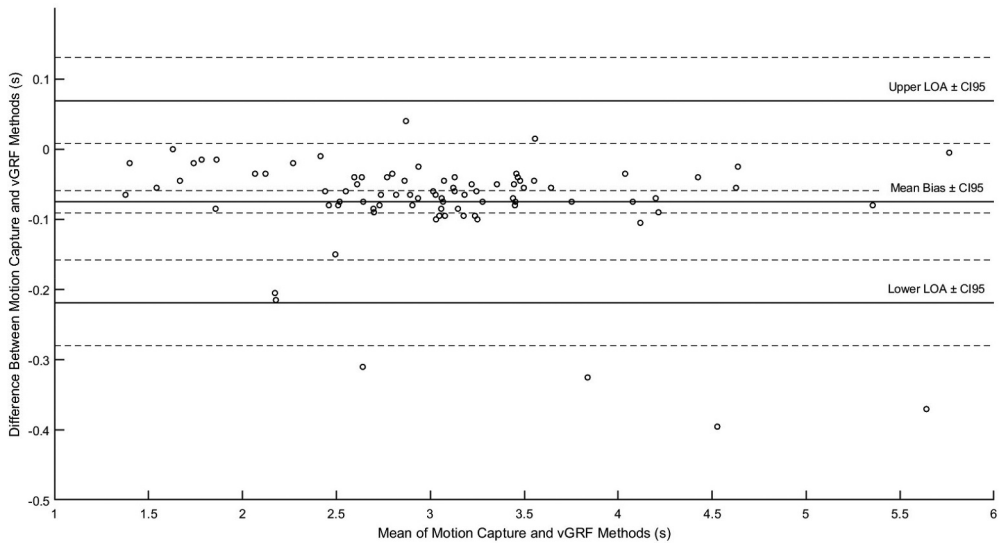


Figure 4. Bland-Altman plot for motion capture and vGRF method of identifying dumbbell release point in CMJ_{AEL20} . The centre line (solid black line) represents the mean bias and the upper (solid black line) and lower (solid black line) limits of agreement are also highlighted. The dashed lines represent upper and lower CI_{95} . Mean, SD and CV% (CI_{95}) values for the motion capture method were 3.03 s, 0.86 s and 5.32 (3.96-8.11), respectively; mean, SD and CV% (CI_{95}) values for the vGRF method were 3.10 s, 0.88 s and 5.27 (3.92-8.03), respectively; mean, SD and CV% (CI_{95}) values for the bottom position were 3.20 s, 0.89 s and 5.22 (3.88-7.95), respectively.

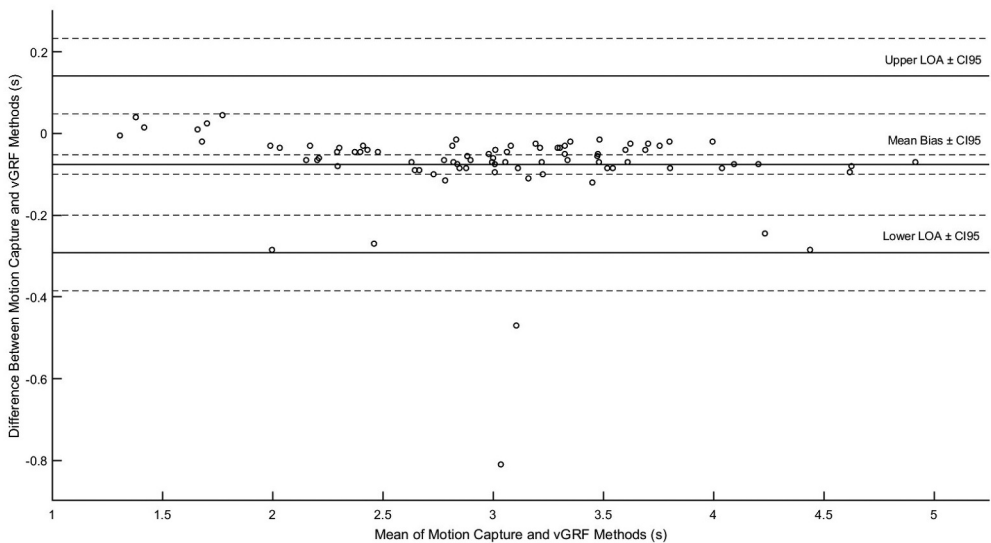


Figure 5. Bland-Altman plot for motion capture and vGRF method of identifying dumbbell release point in CMJ_{AEL30} . The centre line (solid black line) represents the mean bias and the upper (solid black line) and lower (solid black line) limits of agreement are also highlighted. The dashed lines represent upper and lower CI_{95} . Mean, SD and CV% (CI_{95}) values for the motion capture method were 2.96 s, 0.75 s and 4.73 (3.52-7.21), respectively; mean, SD and CV% (CI_{95}) values for the vGRF method were 3.94 s, 0.77 s and 4.76 (3.54-7.25), respectively; mean, SD and CV% (CI_{95}) values for the bottom position were 3.13 s, 0.77 s and 4.58 (3.41-6.98), respectively.

Table 1. Repeated measures Bland-Altman analysis and reliability statistics for motion capture and vGRF methods of identifying the dumbbell release point, in CMJ_{AEL20} and CMJ_{AEL30}.

Condition	Mean Bias (s)	SD of Bias (s)	LOA (s)	Mean Bias \pm CI ₉₅	Lower LOA \pm CI ₉₅	Upper LOA \pm CI ₉₅	CV% (\pm CI ₉₅)	ICC (\pm CI ₉₅)
CMJ _{AEL20}	-0.07	0.07	-0.22, 0.07	-0.09, -0.06	-0.28, -0.16	0.01, 0.13	17.77 (13.14, 27.53)	0.274 (-0.506, 0.707)
CMJ _{AEL30}	-0.08	0.11	-0.29, 0.14	-0.10, -0.05	-0.38, -0.20	0.05, 0.23	13.96 (10.35, 21.48)	0.742 (0.481, 0.894)

SD, standard deviation; LOA, limits of agreement; CI₉₅, 95% confidence intervals; CV%, coefficient of variation percentage; ICC, intraclass correlation coefficient; CMJ_{AEL20}, countermovement jump with accentuated eccentric loading at 20% of body mass; CMJ_{AEL30}, countermovement jump with accentuated eccentric loading at 30% of body mass.

Reliability

Tables 2 and 3 present the reliability data for CMJ_{AEL20} and CMJ_{AEL30}, respectively. System weight and bodyweight were found to have excellent reliability across loading conditions (CV% < 0.10; ICC = 1.000). The DR method elicited moderate-excellent reliability in CMJ_{AEL20} (CV% \leq 7.28; ICC \geq 0.606) and CMJ_{AEL30} (CV% \leq 5.21; ICC \geq 0.797). Moderate-excellent reliability was also observed for the BP method in CMJ_{AEL20} (CV% \leq 12.10; ICC \geq 0.781) and CMJ_{AEL30} (CV% \leq 13.74; ICC \geq 0.791).

CMJ_{AEL} variables

The two-way repeated measures ANOVA revealed significant interaction effects ('method*load') across all variables ($F \geq 10.246$; $p < 0.001$), with the exception of braking force ($F = 0.366$; $p = 0.561$) and braking velocity ($F = 0.134$; $p = 0.741$). For braking force, the main effect of 'method' and 'load' were significant ($F = 60.808$; $p < 0.001$ and $F = 12.110$; $p = 0.003$, respectively). Similarly, for braking velocity, the main effect of 'method' and 'load' were significant ($F = 14.927$; $p < 0.001$ and $F = 4.479$; $p = 0.05$, respectively). The pairwise comparisons and effect sizes are depicted in Tables 4 and 5.

Table 2. Reliability statistics per variable and analysis method for CMJ_{AEL20}.

Variables	Method	CV%	Lower CI ₉₅	Upper CI ₉₅	ICC	Lower CI ₉₅	Upper CI ₉₅
System Weight		0.04	0.03	0.05	1.000	1.000	1.000
Body Weight		0.06	0.04	0.09	1.000	1.000	1.000
Jump Height (m)	BP	8.04	6.03	12.10	0.965	0.930	0.986
	DR	1.18	0.88	1.76	0.997	0.993	0.999
RSI_{mod}	BP	7.90	5.92	11.88	0.963	0.926	0.985
	DR	3.38	2.54	5.08	0.953	0.906	0.981
Displacement (m)	BP	5.24	3.93	7.86	0.891	0.781	0.955
	DR	4.85	3.64	7.28	0.889	0.779	0.954
Force at Zero Velocity (N)	DR	0.88	0.66	1.32	0.997	0.994	0.999
Braking Time (s)	DR	2.50	1.88	3.76	0.952	0.904	0.980
Propulsion Time (s)	DR	3.93	2.95	5.90	0.805	0.606	0.920
Braking Force (N)	DR	0.86	0.65	1.29	0.995	0.991	0.998
Propulsion Force (N)	DR	0.90	0.68	1.35	0.998	0.997	0.999
Braking Mean Velocity (m/s)	BP	2.63	1.98	3.95	0.967	0.932	0.986
	DR	2.21	1.66	3.32	0.965	0.928	0.986
Propulsion Mean Velocity (m/s)	BP	2.97	2.22	4.45	0.989	0.977	0.995
	DR	4.13	3.10	6.20	0.974	0.947	0.989

Note: CV%, coefficient of variation percentage; 95% confidence intervals; ICC, intraclass correlation coefficient; BP, forward integration adjusted at dumbbell release; DR, forward integration adjusted at dumbbell release; RSI_{mod}, reactive strength index modified. Bold numbers indicate unacceptable reliability (Upper CI₉₅ of CV% > 10; lower CI₉₅ of ICC < 0.75).

Table 3. Reliability statistics per variable and analysis method for CMJ_{AEL30}.

Variables	Method	CV%	Lower CI ₉₅	Upper CI ₉₅	ICC	Lower CI ₉₅	Upper CI ₉₅
System Weight		0.04	0.03	0.07	1.000	1.000	1.000
Body Weight		0.06	0.05	0.10	1.000	1.000	1.000
Jump Height (m)	<i>BP</i>	8.99	6.70	13.74	0.896	0.791	0.957
	<i>DR</i>	1.16	0.86	1.77	0.997	0.994	0.999
RSImod	<i>BP</i>	8.88	6.62	13.57	0.955	0.910	0.982
	<i>DR</i>	1.81	1.35	2.75	0.994	0.988	0.998
Displacement (m)	<i>BP</i>	4.25	3.16	6.47	0.924	0.848	0.969
	<i>DR</i>	3.42	2.55	5.21	0.944	0.887	0.977
Force at Zero Velocity (N)	<i>DR</i>	0.89	0.66	1.36	0.997	0.994	0.999
Braking Time (s)	<i>DR</i>	3.08	2.30	4.69	0.908	0.815	0.962
Propulsion Time (s)	<i>DR</i>	2.95	2.20	4.49	0.899	0.797	0.958
Braking Force (N)	<i>DR</i>	1.10	0.82	1.67	0.994	0.989	0.998
Propulsion Force (N)	<i>DR</i>	0.78	0.58	1.19	0.998	0.997	0.999
Braking Mean Velocity (m/s)	<i>BP</i>	2.93	2.18	4.46	0.963	0.925	0.985
	<i>DR</i>	2.90	2.16	4.41	0.958	0.915	0.983
Propulsion Mean Velocity (m/s)	<i>BP</i>	3.78	2.82	5.76	0.971	0.941	0.988
	<i>DR</i>	3.81	2.84	5.80	0.974	0.948	0.989

Note: CV%, coefficient of variation percentage; 95% confidence intervals; ICC, intraclass correlation coefficient; BP, forward integration adjusted at dumbbell release; DR, forward integration adjusted at dumbbell release; RSImod, reactive strength index modified. Bold numbers indicate unacceptable reliability (Upper CI₉₅ of CV% > 10; lower CI₉₅ of ICC < 0.75).

Table 4. Descriptive statistics and effect sizes with 95% confidence intervals for CMJ_{AEL20}.

Variables	Method	Mean	SD	Hedges g (CI ₉₅)		
				<i>BI vs FI</i>	<i>BI vs BP</i>	<i>BI vs DR</i>
Jump Height (m)	<i>BI</i>	0.29	0.11	-2.56 [†]	-0.99 [†]	0.00
	<i>FI</i>	0.07	0.05	(-3.48, -1.64)	(-1.70, -0.27)	(-0.67, 0.67)
	<i>BP</i>	0.19	0.10			
	<i>DR</i>	0.29	0.11			
RSImod	<i>BI</i>	0.36	0.14	-2.48 [†]	-0.99 [†]	0.00
	<i>FI</i>	0.09	0.06	(-3.39, -1.58)	(-1.70, -0.27)	(-0.67, 0.67)
	<i>BP</i>	0.23	0.12			
	<i>DR</i>	0.36	0.14			
Displacement (m)	<i>BI</i>	-0.32	0.09	0.17	0.17	0.47 [†]
	<i>FI</i>	-0.30	0.08	(-0.50, 0.84)	(-0.50, 0.84)	(-0.21, 1.15)
	<i>BP</i>	-0.30	0.08			
	<i>DR</i>	-0.28	0.08			
Force at Zero Velocity (N)	<i>BI</i>	1770.06	492.74	-0.16*		0.00
	<i>FI</i>	1688.30	497.46	(-0.83, 0.51)		(-0.67, 0.67)
	<i>DR</i>	1771.28	489.31			
Braking Time (s)	<i>BI</i>	0.15	0.04	0.91 [†]		0.10*
	<i>FI</i>	0.20	0.05	(0.20, 1.61)		(-0.57, 0.77)
	<i>DR</i>	0.15	0.04			
Propulsion Time (s)	<i>BI</i>	0.28	0.06	-0.67 [†]		-0.07*
	<i>FI</i>	0.24	0.07	(-1.36, 0.02)		(-0.74, 0.61)
	<i>DR</i>	0.28	0.07			
Braking Force (N)	<i>BI</i>	1398.48	352.58	0.17 [†]		0.03 [†]
	<i>FI</i>	1463.18	373.71	(-0.50, 0.85)		(-0.64, 0.71)
	<i>DR</i>	1411.09	357.81			
Propulsion Force (N)	<i>BI</i>	1395.79	417.18	-0.14 [†]		-0.02 [†]
	<i>FI</i>	1335.12	415.92	(-0.82, 0.53)		(-0.69, 0.66)
	<i>DR</i>	1388.66	415.10			
Braking Mean Velocity (m/s ⁻¹)	<i>BI</i>	-0.73	0.16	0.55 [†]	0.56 [†]	0.52 [†]
	<i>FI</i>	-0.65	0.14	(-0.13, 1.24)	(-0.13, 1.24)	(-0.16, 1.21)
	<i>BP</i>	-0.65	0.14			
	<i>DR</i>	-0.65	0.14			
Propulsion Mean Velocity (m/s ⁻¹)	<i>BI</i>	1.51	0.31	-2.35 [†]	-0.87 [†]	0.09 [†]
	<i>FI</i>	0.82	0.27	(-3.24, -1.47)	(-1.58, -0.17)	(-0.58, 0.76)
	<i>BP</i>	1.24	0.31			
	<i>DR</i>	1.54	0.31			

[†]significant difference ($p < 0.001$); *significant difference ($p < 0.05$).

Table 5. Descriptive statistics and effect sizes with 95% confidence intervals for CMJ_{AEL30}.

Variables	Method	Mean	SD	Hedges g (CI ₉₅)		
				BI vs FI	BI vs BP	BI vs DR
Jump Height (m)	BI	0.29	0.11	-3.12 [†]	-1.34 [†]	0.00
	FI	0.03	0.03	(-4.14, -2.10)	(-2.09, -0.59)	(-0.67, 0.67)
	BP	0.13	0.12			
	DR	0.29	0.11			
RSImod	BI	0.35	0.15	-2.83 [†]	-1.42 [†]	0.00
	FI	0.04	0.04	(-3.80, -1.86)	(-2.18, -0.67)	(-0.67, 0.67)
	BP	0.16	0.12			
	DR	0.35	0.15			
Displacement (m)	BI	-0.30	0.11	-0.21	-0.21	0.26*
	FI	-0.33	0.10	(-0.89, 0.46)	(-0.89, 0.46)	(-0.42, 0.93)
	BP	-0.33	0.10			
	DR	-0.28	0.08			
Force at Zero Velocity (N)	BI	1757.58	528.11	-0.27*		0.02
	FI	1614.31	503.71	(-0.95, 0.40)		(-0.65, 0.69)
	BP	1767.45	510.91			
	DR	1767.45	510.91			
Braking Time (s)	BI	0.14	0.05	1.37 [†]		0.00
	FI	0.22	0.06	(0.62, 2.12)		(-0.68, 0.67)
	BP	0.14	0.04			
	DR	0.14	0.04			
Propulsion Time (s)	BI	0.29	0.10	-0.62 [†]		0.00
	FI	0.21	0.14	(-1.31, 0.07)		(-0.67, 0.67)
	BP	0.29	0.13			
	DR	0.29	0.13			
Braking Force (N)	BI	1452.71	389.94	0.16 [†]		0.03 [†]
	FI	1518.82	417.38	(-0.51, 0.83)		(-0.65, 0.70)
	BP	1462.90	395.25			
	DR	1462.90	395.25			
Propulsion Force (N)	BI	1385.69	421.19	-0.27 [†]		-0.01
	FI	1268.24	418.89	(-0.95, 0.40)		(-0.69, 0.66)
	BP	1380.22	416.99			
	DR	1380.22	416.99			
Braking Mean Velocity (m/s ⁻¹)	BI	-0.71	0.20	0.51	0.51	0.49
	FI	-0.62	0.15	(-0.18, 1.19)	(-0.17, 1.19)	(-0.20, 1.17)
	BP	-0.62	0.15			
	DR	-0.62	0.16			
Propulsion Mean Velocity (m/s ⁻¹)	BI	1.48	0.36	-2.89 [†]	-1.26 [†]	0.08 [†]
	FI	0.53	0.28	(-3.87, -1.91)	(-2.00, -0.52)	(-0.60, 0.75)
	BP	1.01	0.37			
	DR	1.51	0.36			

[†]significant difference ($p < 0.001$); *significant difference ($p < 0.05$).

Discussion and implications

The current investigation had two primary aims: (1) to facilitate the quantification of the DBs' release without the need for advanced data acquisition devices (i.e., 3D motion capture) and (2) to provide researchers and practitioners with a method through which they can reliability extract, analyse and interpret force-time variables during a CMJ_{AEL}. It was hypothesised that the 3D motion capture and vGRF methods used to locate the DB release point would agree; however, the agreement between methods was limited by the presence of wide LOA in both loading conditions (CMJ_{AEL20} = -0.22 to 0.07 s; CMJ_{AEL30} = -0.29 to 0.14 s, respectively). In agreement with our second hypothesis, the analysis method (FI, BI, BP and DR) influences both the reliability and magnitude of numerous performance variables during CMJ_{AEL20} and CMJ_{AEL30}. Therefore, depending on which method is deemed to be the criterion method, previous investigations must be interpreted with caution, as fundamental methodological issues may confound the results.

The current consensus on the performance enhancing effects of CMJ_{AEL} are mixed, with studies finding positive (Aboodarda et al., 2013; Sheppard et al., 2007) or negligible and no

effects (Harrison et al., 2019; Taber et al., 2023). Furthermore, our understanding of the mechanisms underpinning CMJ_{AEL} are largely speculative. It is believed that the additional mass and loading of the hip and knee extensors will enhance the ability to store and return elastic strain energy (Bosco et al., 1982; Finni et al., 2001; Hahn et al., 2007; Komi & Gollhofer, 1997), though recent results question this theory (Su et al., 2023a, 2023b). While it is possible that AEL will alter the coordination strategy (i.e., countermovement depth, position of the CoM relative the joints) of a CMJ, any speculated mechanisms that may cause a positive effect rely on the assumption that the additional mass is held throughout the entire countermovement. If this is not the case, it is possible that the hip and knee extensors will be loaded insufficiently, and that the coordination strategy could be affected negatively. It is therefore important that we consider a method by which we can reliably extract the DBs' release point. With this information, researchers and practitioners can make accurate decisions regarding the acute and chronic affects of a CMJ_{AEL} training intervention. For example, if JH decreases, this may be because the athlete is releasing at an inappropriate time in the movement (i.e., too early or too late) and therefore needs more time to familiarise.

The criterion method used to identify the DB release point in this study was 3D motion capture. The DBs were modelled as a rigid segment and their CoM accelerations were calculated and compared with whole body CoM acceleration derived from vGRF (Figure 3). The release point was defined as the first location in which the acceleration of the DB and CoM differed by $\geq 2 \text{ m/s}^2$. This was based on a careful consideration of the study objectives, alongside prior piloting, and the desire to identify a point in the motion where a meaningful deviation between the DB and whole-body CoM acceleration could be reliably detected. This was compared with a vGRF method, which used FI and BI to locate the point in which these signals intersected. The agreement between these methods was unacceptable in both loading conditions; however, it is important to report some additional thoughts. Firstly, the bias threshold used ($\pm 0.05 \text{ s}$) was chosen in absence of established standards in the literature. While it provided a useful benchmark for evaluating agreement, it is important to recognise that it is somewhat arbitrarily designated. Therefore, future research should aim to establish a more definitive threshold. The SD and LOA for CMJ_{AEL20} and CMJ_{AEL30} were large (Figures 4 and 5), suggesting that the difference between methods varied substantially between and within participants (Bland & Altman, 2007). Alongside the poor reliability (Table 1), it could be reasonable to suggest that the vGRF method should not be adopted in future research or practice. However, a deeper examination of the data reveals a different perspective. The motion capture method appears to locate the initiation of the release (i.e., the hand begins to open and the DB acceleration reduces in preparation for release). In contrast, the vGRF method identifies the point at which the DB release is completed, as indicated by the momentary interaction of the FI (system mass) and BI (body mass) signals before they transition to assume each other's magnitude. Considering the need for further analysis of the reliability of the DB release point and potential modifications through coaching (i.e., instructional cues), we propose that the vGRF method could be a viable alternative when 3D motion capture is not feasible. This approach could be particularly beneficial for practitioners already utilising force plate technology to assess their athletes. Given the distinction between these two points and the likely variability in DB release characteristics between participants, it would also be advantageous to model the release as a time period rather than a singular point.

Four separate methods have been presented to calculate CoM acceleration, velocity and displacement (FI, BI, BP and DR). To the best of the authors' knowledge, previous studies have utilised FI (Aboodarda et al., 2013) or BP (Harrison et al., 2019; Taber et al., 2023). A fundamental assumption of FI is that mass remains constant throughout the movement (Street et al., 2001). In CMJ_{AEL} , system mass decreases significantly upon releasing the DBs, rendering FI valid only until this point. To overcome this, researchers have adopted the BP approach, whereby the location of zero velocity (i.e., lowest position) is identified and system mass (body + DB mass) is manually changed to body mass (body mass only) for the remainder of the jump. As mentioned previously, this assumes that the participant releases the additional mass precisely upon reaching their lowest position, something we did not observe in any of our trials. As long as the participant is upright and stands still post-landing, BI, as recently validated (Wade et al., 2022; Wank & Coenning, 2019), can be confidently used to understand performance after the release point of additional mass. Furthermore, once the release point is identified, the FI velocity signal could be more accurately adjusted for the change of mass (i.e., the DR method).

A CMJ is typically de-constructed into phases, defined as the unweighting, braking and propulsion phases (McMahon et al., 2018) or as unloading, eccentric yielding, eccentric braking, and concentric (Harry et al., 2020). Regardless of the phase deconstruction approach, variables based on force, time and velocity are used to describe the performance of each of these phases in relation to the outcome of the jump (i.e., JH). Our findings suggest that variables, with the exception of displacement, extracted from FI are significantly different to those extracted from BI during CMJ_{AEL20} and CMJ_{AEL30} (Tables 4 and 5). Similar comparisons were observed between BI and BP, suggesting that neither FI or BP can be used to extract accurate information beyond the release point. When adjusting mass at a more appropriate location (i.e., DR method), we found the differences to be much less, although still significant for several variables in both loading conditions (Tables 4 and 5). Although comparable reliability was observed between BP and DR methods (Tables 2 and 3), the disparity between BP and BI was considerably larger than that between DR and BI across loading conditions ($g = -1.42$ to 0.56 vs -0.07 to 0.52 , respectively). Given this finding, we recommend the use of the DR method over BP; however, optimal methodology involves combining both FI and BI signals instead of relying on manual adjustments, as the process of manual adjustment necessary for locating the release point is inherently included.

While the results of this study provide some important information regarding the issues with analysing vGRF data from CMJ_{AEL} , it is not without its limitations. For example, the DB release point identified using 3D motion capture was done so via analysis of the CoM and DB segment acceleration data. It is likely that more accurate information could be gathered if markers were placed on the DB and hand; however, this approach was difficult to follow given our experimental set up. Previous work has also explored the use of alternative equipment (i.e., barbells and trap bars) and VJ exercises (i.e., DJ). Future studies should therefore investigate a variety of exercises and equipment to truly understand the utility of AEL during VJ tasks in practice.

Conclusion

The 3D motion capture method and vGRF method should not be used interchangeably to quantify the DB release point during CMJ_{AEL} , as they represent different components

(i.e., initiation of the release and separation, respectively). However, the vGRF method appears to have the potential to locate the point of release when researchers or practitioners only have access to force platforms. A number of studies have reported conflicting findings following CMJ_{AEL}; however, based upon the methods proposed and findings in the current study, the authors discourage the use of FI, BP and DR methods. It is important to note that the aim of the present study was not to discredit previous research but, rather, to build on it with the aim of developing a robust and standardised method of measuring CMJ_{AEL} performance. Therefore, it is proposed that the FI method and BI method are used together, as described in the method section and as shown in [Figure 3](#), to understand performance prior to and after the DBs release, respectively.

Disclosure statement

No potential conflict of interest was reported by the author(s).

ORCID


Thomas E. Bright  <http://orcid.org/0000-0001-8089-817X>

John R. Harry  <http://orcid.org/0000-0002-8207-426X>

Jason Lake  <http://orcid.org/0000-0003-4381-0938>

Peter Mundy  <http://orcid.org/0000-0003-1478-3774>

Nicola Theis  <http://orcid.org/0000-0002-0775-1355>

Jonathan D. Hughes  <http://orcid.org/0000-0002-9905-8055>

References

- Aboodarda, S. J., Byrne, J. M., Samson, M., Wilson, B. D., Mokhtar, A. H., & Behm, D. G. (2014). Does performing drop jumps with additional eccentric loading improve jump performance? *The Journal of Strength & Conditioning Research*, 28(8), 2314. <https://doi.org/10.1519/JSC.0000000000000498>
- Aboodarda, S. J., Yusof, A., Osman, N. A. A., Thompson, M. W., & Mokhtar, A. H. (2013). Enhanced performance with elastic resistance during the eccentric phase of a countermovement jump. *International Journal of Sports Physiology and Performance*, 8(2), 181–187. <https://doi.org/10.1123/ijspp.8.2.181>
- Bland, J. M., & Altman, D. G. (2007). Agreement between methods of measurement with multiple observations per individual. *Journal of Biopharmaceutical Statistics*, 17(4), 571–582. <https://doi.org/10.1080/10543400701329422>
- Bosco, C., Tihanyi, J., Komi, P. V., Fekete, G., & Apor, P. (1982). Store and recoil of elastic energy in slow and fast types of human skeletal muscles. *Acta Physiologica Scandinavica*, 116(4), 343–349. <https://doi.org/10.1111/j.1748-1716.1982.tb07152.x>
- Bridgeman, L., McGuigan, M., Gill, N., & Dulson, D. (2016). The effects of accentuated eccentric loading on the drop jump exercise and the subsequent postactivation potentiation response. *Journal of Strength and Conditioning Research*, 31(6), 1620–1626. <https://doi.org/10.1519/JSC.0000000000001630>
- Bright, T. E., Handford, M. J., Mundy, P., Lake, J., Theis, N., & Hughes, J. D. (2023). Building for the future: A systematic review of the effects of eccentric resistance training on measures of physical performance in youth athletes. *Sports Medicine*, 53(6), 1219–1254. <https://doi.org/10.1007/s40279-023-01843-y>

- Burnett, J. K., Kim, Y.-W., Kwon, H. J., Miller, R. H., & Shim, J. K. (2023). Whole body mass estimates and error propagation in countermovement jump: A simulated error study. *Sports Biomechanics*, 1–14. <https://doi.org/10.1080/14763141.2023.2236589>
- Cohen, J. (2009). *Statistical power analysis for the behavioral sciences* (2 ed. reprint). Psychology Press.
- Finni, T., Ikegawa, S., & Komi, P. V. (2001). Concentric force enhancement during human movement. *Acta Physiologica Scandinavica*, 173(4), 369–377. <https://doi.org/10.1046/j.1365-201X.2001.00915.x>
- Frayne, D. H., Zettel, J. L., Beach, T. A. C., & Brown, S. H. M. (2021). The influence of countermovements on inter-segmental coordination and mechanical energy transfer during vertical jumping. *Journal of Motor Behavior*, 53(5), 545–557. <https://doi.org/10.1080/00222895.2020.1810611>
- Gard, S. A., Miff, S. C., & Kuo, A. D. (2004). Comparison of kinematic and kinetic methods for computing the vertical motion of the body center of mass during walking. *Human Movement Science*, 22(6), 597–610. <https://doi.org/10.1016/j.humov.2003.11.002>
- Gross, M., Seiler, J., Grédy, B., & Lüthy, F. (2022). Kinematic and kinetic characteristics of repetitive countermovement jumps with accentuated eccentric loading. *Sports*, 10(5), Article 5. <https://doi.org/10.3390/sports10050074>
- Grozier, C. D., Cagle, G. K., Pantone, L., Rank, K. B., Wilson, S. J., Harry, J. R., Seals, S., & Simpson, J. D. (2021). Effects of medial longitudinal arch flexibility on propulsion kinetics during drop vertical jumps. *Journal of Biomechanics*, 118, 110322. <https://doi.org/10.1016/j.jbiomech.2021.110322>
- Hahn, D., Seiberl, W., & Schwirtz, A. (2007). Force enhancement during and following muscle stretch of maximal voluntarily activated human quadriceps femoris. *European Journal of Applied Physiology*, 100(6), 701–709. <https://doi.org/10.1007/s00421-007-0462-3>
- Hamilton, C., & Stamey, J. (2007). Using Bland–Altman to assess agreement between two medical devices – Don't forget the confidence intervals! *Journal of Clinical Monitoring and Computing*, 21(6), 331–333. <https://doi.org/10.1007/s10877-007-9092-x>
- Handford, M. J., Rivera, F. M., Maroto-Izquierdo, S., & Hughes, J. D. (2021). Plyo-Accentuated eccentric loading methods to enhance lower limb muscle power. *Strength & Conditioning Journal*, 43(5), 54. <https://doi.org/10.1519/SSC.0000000000000635>
- Harrison, A. J., Byrne, P., & Sundar, S. (2019). The effects of added mass on the biomechanics and performance of countermovement jumps. *Journal of Sports Sciences*, 37(14), 1591–1599. <https://doi.org/10.1080/02640414.2019.1577120>
- Harry, J. R., Barker, L. A., & Paquette, M. R. (2020). A joint power approach to define countermovement jump phases using force platforms. *Medicine and Science in Sports and Exercise*, 52(4), 993–1000. <https://doi.org/10.1249/mss.00000000000002197>
- Harry, J. R., Blinck, J., Barker, L. A., Krzyszkowski, J., & Chowning, L. (2022). Low-pass filter effects on metrics of countermovement vertical jump performance. *Journal of Strength and Conditioning Research*, 36(5), 1459–1467. <https://doi.org/10.1519/JSC.0000000000003611>
- Hyslop, N. P., & White, W. H. (2009). Estimating precision using duplicate measurements. *Journal of the Air & Waste Management Association*, 59(9), 1032–1039. <https://doi.org/10.3155/1047-3289.59.9.1032>
- Kibele, A. (1998). Possibilities and limitations in the biomechanical analysis of countermovement jumps: A methodological study. *Journal of Applied Biomechanics*, 14(1), 105–117. <https://doi.org/10.1123/jab.14.1.105>
- Komi, P. V., & Gollhofer, A. (1997). Stretch reflexes can have an important role in force enhancement during SSC exercise. *Journal of Applied Biomechanics*, 13(4), 451–460. <https://doi.org/10.1123/jab.13.4.451>
- Koo, T. K., & Li, M. Y. (2016). A guideline of selecting and reporting intraclass correlation coefficients for reliability research. *Journal of Chiropractic Medicine*, 15(2), 155–163. <https://doi.org/10.1016/j.jcm.2016.02.012>
- Lloyd, R. S., Howard, S. W., Pedley, J. S., Read, P. J., Gould, Z. I., & Oliver, J. L. (2022). The acute effects of accentuated eccentric loading on drop jump kinetics in adolescent athletes. *Journal of*

- Strength and Conditioning Research*, 36(9), 2381–2386. <https://doi.org/10.1519/JSC.0000000000003911>
- McMahon, J. J., Suchomel, T. J., Lake, J. P., & Comfort, P. (2018). Understanding the key phases of the countermovement jump force-time curve. *Strength & Conditioning Journal*, 40(4), 96. <https://doi.org/10.1519/SSC.0000000000000375>
- Merrigan, J., Borth, J., Taber, C., Suchomel, T., & Jones, M. (2022). Application of accentuated eccentric loading to elicit acute and chronic velocity and power improvements: A narrative review. *International Journal of Strength and Conditioning*, 2(1), Article 1. <https://doi.org/10.47206/ijsc.v2i1.80>
- Owen, N. J., Watkins, J., Kilduff, L. P., Bevan, H. R., & Bennett, M. A. (2014). Development of a criterion method to determine peak mechanical power output in a countermovement jump. *The Journal of Strength & Conditioning Research*, 28(6), 1552. <https://doi.org/10.1519/JSC.0000000000000311>
- Psycharakis, S. G., & Miller, S. (2006). Estimation of errors in force platform data. *Research Quarterly for Exercise and Sport*, 77(4), 514–518. <https://doi.org/10.1080/02701367.2006.10599386>
- Quagliarella, L., Sasanelli, N., & Monaco, V. (2008). Drift in posturography systems equipped with a piezoelectric force platform: Analysis and numerical compensation. *IEEE Transactions on Instrumentation and Measurement*, 57(5), 997–1004. <https://doi.org/10.1109/TIM.2007.913833>
- Sheppard, J., Newton, R., & McGuigan, M. (2007). The effect of accentuated eccentric load on jump kinetics in high-performance volleyball players. *International Journal of Sports Science & Coaching*, 2(3), 267–273. <https://doi.org/10.1260/174795407782233209>
- Street, G., McMillan, S., Board, W., Rasmussen, M., & Heneghan, J. M. (2001). Sources of error in determining countermovement jump height with the impulse method. *Journal of Applied Biomechanics*, 17(1), 43–54. <https://doi.org/10.1123/jab.17.1.43>
- Su, E. Y.-S., Carroll, T. J., Farris, D. J., & Lichtwark, G. A. (2023a). Musculoskeletal simulations to examine the effects of accentuated eccentric loading (AEL) on jump height. *PeerJ*, 11, e14687. <https://doi.org/10.7717/peerj.14687>
- Su, E. Y.-S., Carroll, T. J., Farris, D. J., & Lichtwark, G. (2023b). Increased force and elastic energy storage are not the mechanisms that improve jump performance with accentuated eccentric loading during a constrained vertical jump. *bioRxiv*. <https://doi.org/10.1101/2023.10.30.564851>
- Taber, C., Butler, C., Dabek, V., Kochan, B., McCormick, K., Petro, E., Suchomel, T., & Merrigan, J. (2023). The effects of accentuated eccentric loading on barbell and trap bar countermovement jumps. *International Journal of Strength and Conditioning*, 3(1), Article 1. <https://doi.org/10.47206/ijsc.v3i1.213>
- Wade, L., Needham, L., Evans, M., McGuigan, P., Colyer, S., Cosker, D., Bilzon, J., & Gu, Y. (2023). Examination of 2D frontal and sagittal markerless motion capture: Implications for markerless applications. *PLOS ONE*, 18(11), e0293917. <https://doi.org/10.1371/journal.pone.0293917>
- Wade, L., Needham, L., McGuigan, M. P., & Bilzon, J. L. J. (2022). Backward double integration is a valid method to calculate maximal and sub-maximal jump height. *Journal of Sports Sciences*, 40(10), 1191–1197. <https://doi.org/10.1080/02640414.2022.2059319>
- Wagle, J. P., Taber, C. B., Cunanan, A. J., Bingham, G. E., Carroll, K. M., DeWeese, B. H., Sato, K., & Stone, M. H. (2017). Accentuated eccentric loading for training and performance: A review. *Sports Medicine*, 47(12), 2473–2495. <https://doi.org/10.1007/s40279-017-0755-6>
- Wank, V., & Coenning, C. (2019). On the estimation of centre of gravity height in vertical jumping. *German Journal of Exercise and Sport Research*, 49(4), 454–462. <https://doi.org/10.1007/s12662-019-00581-6>
- Wiesinger, H.-P., Rieder, F., Kösters, A., Müller, E., & Seynnes, O. R. (2017). Sport-specific capacity to use elastic energy in the patellar and achilles tendons of elite athletes. *Frontiers in Physiology*, 8, 8. <https://doi.org/10.3389/fphys.2017.00132>
- Zok, M., Mazzà, C., & Della Croce, U. (2004). Total body centre of mass displacement estimated using ground reactions during transitory motor tasks: Application to step ascent. *Medical Engineering & Physics*, 26(9), 791–798. <https://doi.org/10.1016/j.medengphy.2004.07.005>